Journal of Hydrology 574 (2019) 936–945

Contents lists available at ScienceDirect

Journal of Hydrology

journal homepage: www.elsevier.com/locate/jhydrol

Research papers

Quantifying the relative contribution of climate and human impacts on seasonal streamflow

Zhuohang Xin, Yu Li*, Lu Zhang, Wei Ding, Lei Ye, Jian Wu, Chi Zhang

School of Hydraulic Engineering, Dalian University of Technology, Dalian 116024, China

ARTICLE INFO

This manuscript was handled by Dr marco borga, Editor-in-Chief

Keywords:
Climate change
Human activities
Streamflow
Budyko-type equation
Abcd model
Reservoir operation

ABSTRACT

Climate change and human activities have induced alterations to hydrological processes. The quantification of their impacts on streamflow is a challenge, especially at the seasonal scale due to seasonality of climate variables and human activities. In this study, the decomposition method based on Budyko equation is extended to the seasonal scale for quantifying the climate and direct human impacts on annual and seasonal streamflow changes in Huifa River basin by defining prechange period (1953–1974) and postchange period (1975–2005). The results are further verified by the monthly abcd model. Both climate change and direct human activities are found to induce a decrease in streamflow at the annual scale, with 68% of the change contributed by direct human activities. At the seasonal scale, the direct human-induced declines in streamflow account for 67% and 39% of the total changes for energy-limited and water-limited seasons, respectively; whereas, the impact of direct human activities is more pronounced during the irrigation season due to water withdrawal for irrigation. In addition, the decomposition results are analyzed for each month in the energy-limited season to reveal the effects of precipitation and operation rules of ponds and reservoirs during the flood season.

1. Introduction

Climate change and human activities are two major drivers that alter hydrological cycle and have exerted global-scale impacts on environment with significant implications for water resources management (Jaramillo and Destouni, 2014, 2015; Kundzewicz et al., 2008; Milly et al., 2008; Vogel, 2011). Climate change including precipitation and potential evaporation causes significant alterations in streamflow and evapotranspiration (Dooge, 1992). Human activities can influence the streamflow directly by disturbing the hydrological processes (such as land use change, dam construction, reservoir operation, surface water and groundwater withdrawals and return flows), or indirectly by affecting the climate variables (such as elevated CO_2 and O_3 concentrations, urban heat island, irrigation, and crop evapotranspiration) (Arrigoni et al., 2010; McLaughlin et al., 2007; Rossi et al., 2009; Wang and Cai, 2010). Significant changing trends have been detected in streamflow for many rivers around the world (Jiang et al., 2015; Vaze et al., 2011; Xu et al., 2014). The research interests of quantifying the contribution of climate change and human activities on streamflow have increased in past decades due to the important roles of streamflow in water uses for agriculture, domestic, industry, hydropower generation and navigation.

Many studies have been focused on quantifying the impacts of climate change and human activities on streamflow based on streamflow elasticity, distributed or conceptual hydrological models. The elasticity method initially proposed by Schaake (1990) uses elasticity coefficients to represent the sensitivity of streamflow to changes in precipitation, and then has been improved by many scholars. The elasticity of streamflow to various climate variables have been quantified, such as precipitation (Niemann and Eltahir, 2005; Sankarasubramanian et al., 2001; Sun et al., 2013), temperature (Fu et al., 2007; Ma et al., 2010), relative humidity (Dooge et al., 1999), and potential evaporation (Liu et al., 2013; Tang and Lettenmaier, 2012). For example, Yang and Yang (2011) derived climate elasticity of streamflow to precipitation, temperature, wind speed, relative humidity and net radiation. The elasticity coefficients have been estimated by a nonparametric method (Ma et al., 2010; Sankarasubramanian et al., 2001) or a Budyko equation (Arora, 2002; Dooge et al., 1999; Xu et al., 2014). The challenge of elasticity method is to explicitly compute the elasticity coefficients of streamflow to human activities (Sun et al., 2014).

For the method based on hydrological models, the impact of one specific contributor (climate or human) on streamflow is evaluated by changing the parameter for the contributor while fixing other parameters (Bao et al., 2012; Dey and Mishra, 2017; Sun et al., 2014; Wang et al., 2013). The hydrological models used for this purpose include the

* Corresponding author.
E-mail address: liyu@dlut.edu.cn (Y. Li).

https://doi.org/10.1016/j.jhydrol.2019.04.095
Received 1 February 2018; Received in revised form 12 March 2019; Accepted 30 April 2019
Available online 03 May 2019

SWAT (Soil Water Assessment Tool) (Li et al., 2009; Mango et al., 2011; Zhang, 2013), DTVGM (Distributed time-variant gain model) (Wang et al., 2009), GBHM (Geomorphology-Based Hydrological Model) (Ma et al., 2010), and VIC (Variable Infiltration Capacity) model (Liu et al., 2013; Xu et al., 2013). Wang and Hejazi (2011) proposed the decomposition method based on a conceptual hydrologic model, i.e., Budyko equation, for quantifying the contributions of climate change and direct human activities to mean annual streamflow explicitly. The decomposition method has been recently applied and extended to watersheds in China (Jiang et al., 2015; Sun et al., 2014).

Previous studies are mostly focused on separating the attribution of climate change and human activities to annual streamflow changes. However, few attempts were devoted to streamflow at a shorter time scale, such as seasonal or monthly scale. Such studies are essential due to the intra-annual variations of hydro-climatic variables and human activities, such as rainfall seasonality, intense water withdrawals during irrigation periods, and reservoir operations during flood season (Bao et al., 2012; Zhang and Wang, 2014; Liang et al., 2015).

This paper aims to quantify the contributions of climate change and human activities to intra-annual streamflow changes at seasonal scale. The decomposition method based on Budyko equation is extended to the seasonal scale by introducing a seasonal aridity index (Chen et al., 2013). The proposed framework is then employed to the Huifa River basin in China, which has suffered from climate change and human interferences during the past decades. The impacts of intra-annual human activities (e.g., water withdrawal for irrigation, water storage and release by ponds and reservoirs) on streamflow are quantified. Moreover, the quantification results are compared with the simulation of a monthly water balance model (i.e., abcd model).

2. Methodology

2.1. Decomposition method based on extended Budyko-type model

The semi-empirical equation proposed by Budyko (1974) is a non-parametric model for long-term water balance (Donohue et al., 2010). To incorporate the seasonal effects on water balance, the water storage dynamics needs to be considered; that is, watershed storage can be depleted in the water-limited seasons and replenished by infiltrated precipitation in the energy-limited seasons. Therefore, the water storage change needs to be subtracted from precipitation for accounting the available water supply, which is defined as effective precipitation (P-ΔS) (Chen et al., 2013; Wang, 2012). Correspondingly, the seasonal aridity index is defined as the ratio of seasonal potential evaporation to seasonal effective precipitation, and the seasonal evaporation ratio is defined as the ratio between seasonal evaporation and seasonal effective precipitation. Considering that the seasonal aridity index for a given watershed may be a positive value, a shift along the horizontal axis is introduced to characterize the nonzero lower bound. The modified Budyko-type equation (Choudhury, 1999; Mezentsev, 1955; Yang et al., 2008a) is used to model the dependence of seasonal evaporation ratio on seasonal aridity index (Chen et al., 2013).

$$\frac{E}{P-\Delta S}=\left[1+\left(\frac{E_p}{P-\Delta S}-\varphi\right)^{-n}\right]^{-\frac{1}{n}} \tag{1}$$

where E, E_p and P are seasonal values for evaporation, potential evaporation and precipitation, respectively; ΔS is seasonal water storage change, including soil water and groundwater storage changes; n is the parameter representing the effects of other factors such as vegetation, soil and topography on the partition of precipitation that determines the shape of the Budyko curve; and φ is the lower bound for seasonal aridity index.

By utilizing the decomposition method proposed by Wang and Hejazi (2011), the climate-induced and direct human-induced changes in streamflow are quantified at the seasonal scale. In this method, the

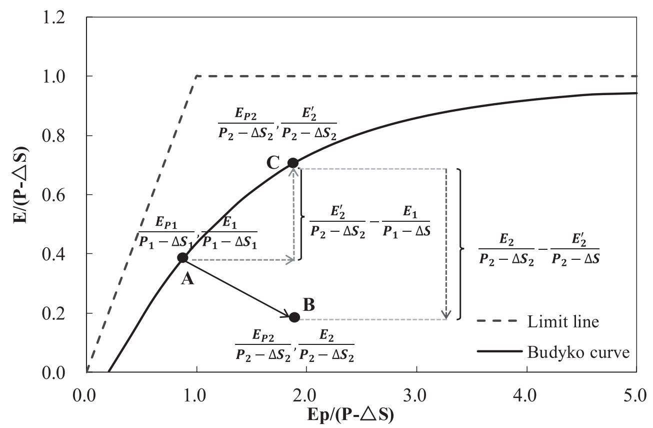

Fig. 1. Schematic of Budyko-type decomposition method to quantify the climate and direct human impacts on streamflow change at seasonal scale.

climate change or variability refers to the alterations of effective precipitation and potential evaporation which can be due to natural climate variability, global climate change, and the regional and local climate effects due to human activities. The direct human impact represents the change of effective precipitation portioning into evaporation and streamflow under given climate conditions; it does not include the indirect human impacts that affect the streamflow through disturbing the climate variability (Wang and Hejazi, 2011). The schematic of the decomposition method is shown in Fig. 1. To evaluate the change, the study period is split into two sub-periods, namely the prechange and postchange periods. The prechange period is the baseline, and climate change and direct human activities may contribute to streamflow change in the postchange period.

At the seasonal scale, the Budyko equation quantifies the partitioning of precipitation into runoff, evaporation, and water storage change. The proposed decomposition method assumes that for a watershed without direct human impact, if climate $\left(\frac{E_p}{P-\Delta S}\right)$ is changed to a drier or wetter condition due to climate change or variability, the evaporation ratio $\left(\frac{E_p}{P-\Delta S}\right)$ will also change to a new state but still follow the original Budyko curve as the prechange period. This assumption is considered reasonable because the shape of Budyko-type curve is largely dependent on the physical properties of watersheds, such as soil properties, vegetation characteristics, and topography (Wang and Wu, 2013; Yang et al., 2007); and these properties, especially the natural vegetation dynamics co-evolve with the climate variability and change through evaporation and water storage (Jones, 2011; Sivapalan, 2006). Therefore, the movement of a watershed along the horizontal direction (i.e., change of$\frac{E_p}{P-\Delta S}$) is driven by climate change or variability; the movement along the vertical direction (i.e., change of $\frac{E_p}{P-\Delta S}$ due to change of E) can be attributed to both climate and direct human impacts.

As shown in Fig. 1, a watershed shifts over time from point A $\left(\frac{E_{p1}}{P_1-\Delta S_1}, \frac{E_1}{P_1-\Delta S_1}\right)$ in the prechange period to point B $\left(\frac{E_{p1}}{P_1-\Delta S_1}, \frac{E_1}{P_1-\Delta S_1}\right)$ in the postchange period. If only affected by climate change or variability, the watershed will evolve from point A to C $\left(\frac{E_{p2}}{P_2-\Delta S_2}, \frac{E_2'}{P_2-\Delta S_2}\right)$ along the original Budyko curve, where point C is a hypothetical point that has the same climate condition as point B. Therefore, climate change induces both horizontal and vertical changes, i.e., from $\frac{E_{p1}}{P_1-\Delta S_1}$ to $\frac{E_{p2}}{P_2-\Delta S_2}$ along the horizontal direction and from $\frac{E_1}{P_1-\Delta S_1}$ to $\frac{E_2'}{P_2-\Delta S_2}$ along the vertical direction; whereas direct human impacts move watersheds along the vertical direction from $\frac{E_2'}{P_2-\Delta S_2}$ to $\frac{E_2}{P_2-\Delta S_2}$. The direct human-induced change of streamflow (ΔQ_h) is computed by:

$$\Delta Q_h=(P_2-\Delta S_2)\left(\frac{E_2'}{P_2-\Delta S_2}-\frac{E_2}{P_2-\Delta S_2}\right) \tag{2}$$

where ΔQ_h is the direct human-induced streamflow change in the postchange period. Then, the climate-induced change of streamflow (ΔQ_c) is the remaining component calculated by subtracting the human-induced change from the total streamflow change (ΔQ):

$$\Delta Q_c = \Delta Q - \Delta Q_h \tag{3}$$

where ΔQ is the difference in streamflow between the postchange (Q_2) and prechange (Q_1) periods:

$$\Delta Q = Q_2 - Q_1 \tag{4}$$

where Q_1 and Q_2 are observed streamflow during the prechange and postchange periods, respectively.

Given the time series of precipitation, streamflow, and meteorological data, the decomposition method is implemented with the following steps:

(1) The monthly E_p is calculated using Penman-Monteith (PM) equation (Allen et al., 1998).
(2) Given the monthly precipitation and potential evaporation, the actual evaporation and water storage change are estimated for the prechange and postchange periods using the abcd model. Details on the abcd model and its extension are explained in Sections 2.2.
(3) The monthly data from Step (1) and Step (2) are aggregated to seasonal and annual averages, and the corresponding evaporation ratio and aridity index, i.e., $\frac{E_1}{P_1 - \Delta S_1}$ and $\frac{E_{p1}}{P_1 - \Delta S_1}$ for the prechange period and $\frac{E_2}{P_2 - \Delta S_2}$ and $\frac{E_{p2}}{P_2 - \Delta S_2}$ for the postchange period, are computed.
(4) The parameters of φ and n in Eq. (1) are calibrated to $\frac{E_1}{P_1 - \Delta S_1}$ and $\frac{E_{p1}}{P_1 - \Delta S_1}$ for the prechange period; that is, different Budyko curves are fitted for the annual scale, irrigation season, energy-limited season, and water-limited season, respectively.
(5) In the postchange period, the evaporation ratio due to climate change only $\left(\frac{E_2'}{P_2 - \Delta S_2}\right)$ is calculated based on the calibrated parameters (φ and n) in Step (4) and seasonal aridity index ($\frac{E_{p2}}{P_2 - \Delta S_2}$) in Step (3).
(6) The climate- and direct human–induced changes in streamflow can be computed by Eqs. (2)–(4).

To deal with the uncertainty of E_p estimation, the Hargreaves and Samani (HS) method (Hargreaves and Samani, 1985) is also applied for estimating E_p; the quantification results by repeating steps (1)–(6) are presented in Sections 4.4 and 4.5.

2.2. Monthly abcd model

The monthly abcd model takes precipitation and potential evaporation as input, captures the dynamics of soil moisture and groundwater, and produces streamflow as output (Thomas, 1981). In the abcd model, the equation for quantifying the partitioning of the sum of precipitation and initial storage can be derived from the generalized proportionality relation of SCS curve number method (Wang and Tang, 2014). This model has been used in many studies (e.g., Alley, 1984; Fernandez et al., 2000), and the details of the model can be found in previous studies, such as Alley (1984) and Sankarasubramanian and Vogel (2002).

The model includes four parameters (i.e., *a, b, c* and *d*). Parameter *a* ($0 \le a \le 1$) reflects the propensity of runoff to occur before the soil is fully saturated (Thomas, 1981); parameter *b* is an upper limit of the sum of evapotranspiration and soil moisture storage; parameter *c* is the fraction of streamflow from groundwater discharge; and parameter *d* is the coefficient for groundwater storage-discharge relation. These four parameters, as well as the initial soil water storage (between 0 and *b*), were subject to calibration, and the initial groundwater storage was determined by the method proposed by Alley (1984). In addition to these processes considered in the abcd model, this study applied the degree-day model to take into account the effects of snow storage and snowmelt. If the daily mean air temperature is below 0 °C, the precipitation, either by snow or rainfall is assumed to be temporarily stored as ice/snow pack on the ground rather than converting to stream flows (Braithwaite and Zhang, 2000; Wu et al., 2011); otherwise the ice/snowmelt occurs which may provide additional inputs to the streamflow. The amount of ice/snowmelt is calculated by empirically relating to the mean daily air temperature (Hock, 2003, 2005; Yang, 2015), and the melt amount is added to precipitation in the abcd model rather than directly discharged into the water body.

Given the time series of precipitation and potential evaporation, the model was calibrated to the measured streamflow with the help of a genetic algorithm. An objective function *O* is used for evaluating the model performance, which is defined on the basis of Nash-Sutcliffe efficiency coefficient (*NSE*) and coefficient of determination (R^2):

$$O = \lambda(1 - NSE) + (1 - \lambda)(1 - R^2) \tag{5}$$

where λ is the weighting factor taken as 0.5. The smaller the value of *O*, the better the model performance.

In this study, the abcd model is applied mainly with two purposes. First, the model parameters are calibrated to the measured streamflow in both prechange and postchange periods; the monthly actual evaporation and water storage change can be solved numerically at the same time using the calibrated parameters and derived model equations (Sankarasubramanian and Vogel, 2002), which are further used to calculate the seasonal evaporation ratio and seasonal aridity index for both periods in the Budyko decomposition method. Second, to validate the proposed Budyko decomposition method, the abcd model was applied for quantifying the climate and human impacts on streamflow change as a comparison. In this case, the prechange period is the benchmark, and the streamflow in the postchange period under climate change impact only (Q_{sim2}) is produced using the calibrated parameters from the prechange period and the climate conditions in the postchange period. The human-induced streamflow change in the postchange period (ΔQ_h) can be calculated by

$$\Delta Q_h = Q_2 - Q_{sim2} \tag{6}$$

The climate-induced change in streamflow for the postchange period can be computed by Eqs. (3) and (4). All data are initially generated on a monthly basis and further aggregated to obtain the seasonal and annual averages.

2.3. Seasonality identification

Considering the seasonal variation of climate variables, watershed properties and human activities (Bao et al., 2012; Yang et al., 2008b), the energy-limited and water-limited seasons within one hydrological year need to be identified. Chen et al. (2013) proposed a method to define the energy-limited and water-limited months by introducing the monthly aridity index, A_m. To define fixed energy-limited and water-limited months over the entire period for the study region, the mean monthly aridity index is used:

$$\bar{A}_m = \frac{\bar{E}_{pm}}{\bar{P}_m - \bar{\Delta S}_m} \tag{7}$$

where $\bar{E}_{pm}$, $\bar{P}_m$, $\bar{\Delta S}_m$ are averaged monthly potential evaporation, precipitation, and storage change, respectively. The energy-limited and water-limited months are differentiated by a threshold value of $\bar{A}_m = 1$: months with $\bar{A}_m \ge 1$ are identified as water-limited, and months with $\bar{A}_m < 1$ are identified as energy-limited. The two seasons are defined by aggregating the identified energy-limited and water-limited months.

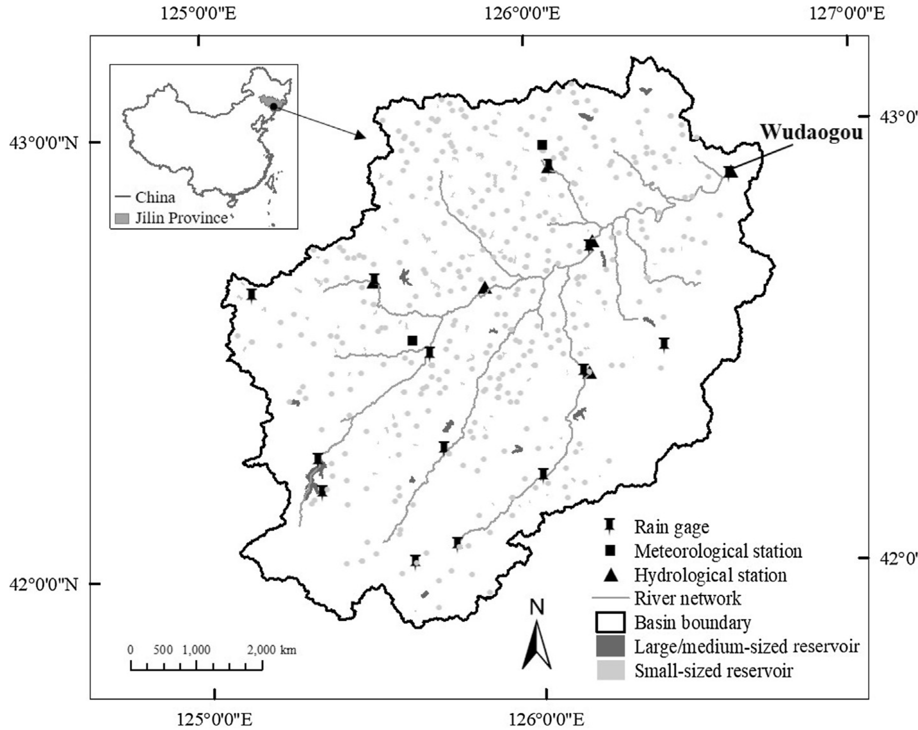

Fig. 2. Map of the Huifa River basin showing the river system, and locations of hydrological and meteorological stations and reservoirs.

3. Study area and data

3.1. Study area

This study is focused on the Huifa River basin (Fig. 2), which is located in the south area of Jilin Province, China. The Huifa River is a major tributary of the second Songhua River with a total length of 268 km. It originates from the Longgang mountain ranges and flows northeast into the second Songhua River. The total basin area is about 12,411 km^2 with 43% of forest and 35% of farmland in 2012. The area has a semi-humid climate featured with distinguished seasons. The mean annual precipitation is about 720 mm, with more than 70% of precipitation occurring during the flood season from July to September. The mean annual air temperature is about 5.5 °C. December to February are the coldest months with a mean monthly temperature of −12.5 °C, and July is the warmest month with a mean temperature of 22.6 °C. Precipitation mainly occurs as snow from November to February, and ice/snowmelt normally starts in March.

In the past few decades, the Huifa River basin has suffered from significant anthropogenic influences, and becomes one of the heavily urbanized areas in Jilin Province. Specifically, many water conservation projects have been constructed to meet the water demand for domestic use and irrigation under the pressures of population growth and irrigation. There are one large-scale reservoir, hundreds of small to medium-scale reservoirs, and countless ponds in the study area, and the total storage capacity is about 9.5×10^8 m^3. The total drainage area of all water conservation projects is about 7500 km^2, covering up to 64% of the total area (Zhang et al., 2012).

3.2. Data

Daily precipitation data at nine rain gauge stations were provided by the Hydrological Bureau of Jilin Province, and the spatial averages were used. Daily streamflow data at the downstream Wudaogou hydrological station was collected from the Songliao Water Resources Commission, Ministry of Water Resources. Meteorological conditions including relative humidity, wind speed, sunshine duration, and mean, minimum and maximum air temperatures on a daily basis at three meteorological stations were downloaded from the China Meteorological Data Service Center (http://data.cma.cn/), and the spatial averages were further computed. All data cover a period from 1953 to 2005. The locations of all the stations are shown in Fig. 2.

4. Results and discussion

4.1. Trend of hydro-meteorological series and breakpoint

The nonparametric Mann-Kendall test (Kendall, 1975; Mann, 1945) is implemented to detect the trend of annual precipitation, streamflow and potential evaporation from 1953 to 2005. As shown in Table 1, the annual streamflow presents a significant decreasing trend that passes the trend test at the 0.01 significance level. Precipitation and potential evaporation also show some degree of decreasing trend, but not significant. Fig. 3 presents the annual and 5-year moving averages of streamflow, precipitation and potential evaporation. The variation trend is consistent with the Mann-Kendall test, showing a changing rate of −2.11 mm/year, −1.35 mm/year and −0.38 mm/year on average for streamflow, precipitation and potential evaporation, respectively.

The cumulative double mass method (Searcy and Hardison, 1960; Xue et al., 2017) and Pettitt test (Pettitt, 1979) are used to identify the breakpoint of streamflow for determining the prechange and post-change periods. Fig. 4 shows the relationship between cumulative annual streamflow versus cumulative annual precipitation. It is apparent that the year 1975 can be identified as a breakpoint since the

Table 1
Results of Mann-Kendall trend test for streamflow, precipitation and potential evaporation.

Variable	$Z_{mann\text{-}kendall}$
Streamflow	−2.75*
Precipitation	−0.28
Potential evaporation	−0.06

* Trend is significant at the significance level of 0.01.

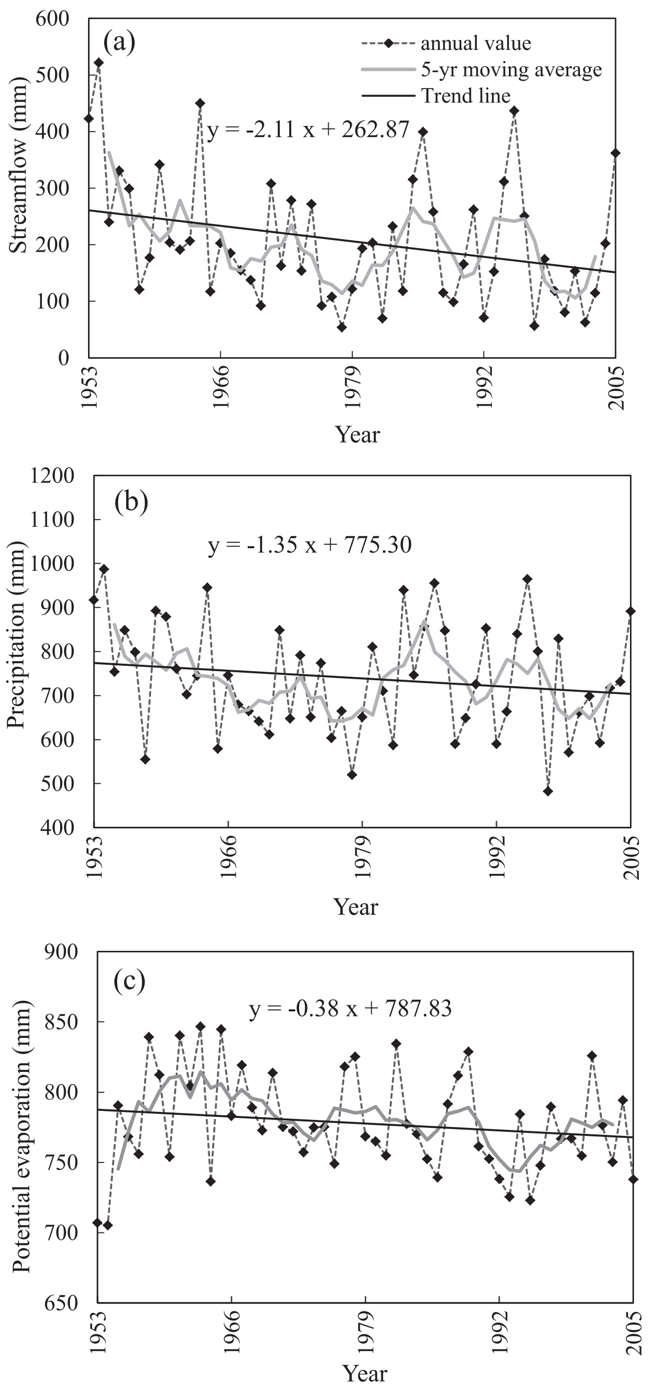

Fig. 3. Annual variations of (a) streamflow, (b) precipitation and (c) potential evaporation for the Huifa River basin from 1953 to 2005.

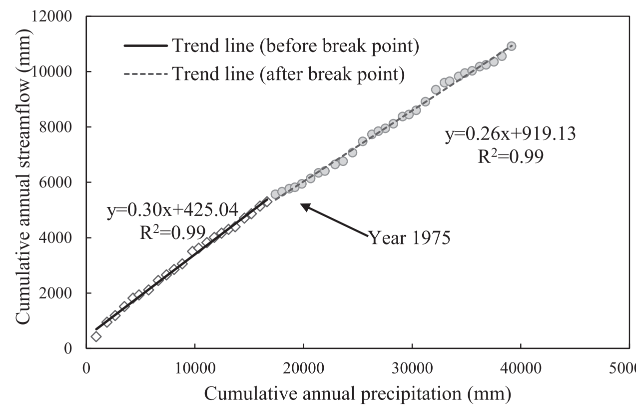

Fig. 4. Cumulative annual streamflow versus cumulative annual precipitation from 1953 to 2005.

correlations before and after the point are significantly different, with the slopes of regression lines being 0.30 and 0.26, respectively. Meanwhile, the Pettitt test proved the same breakpoint in 1975 at a significance level of 0.02. The breakpoint determined in this study is in accordance with the year suggested by Zhang (2013) for the same study region. In addition, a large number of water conservation projects in the study region were constructed during 1960s–1970s, indicating an emergence of human activities during that period. Once the breakpoint is detected, the overall time series is split into two sub-periods, the prechange period from 1953 to 1974 and the postchange period from 1975 to 2005.

4.2. Fitting results of Budyko-type model

According to the definition of energy-limited and water-limited months explained in Section 2.3, the energy-limited and water-limited seasons in this study region are identified as July to September, and October to June, respectively. In addition, an irrigation period is defined as May to July due to water withdrawal for irrigation. Therefore, there are water-limited season (October to April), irrigation season (May to July), and energy-limited season (July to September) in this study.

Fig. 5 plots the correlations of evaporation ratio versus aridity index for the prechange and postchange periods for annual scale, irrigation season, energy-limited season, and water-limited season, respectively. The two parameters (n and φ) in the seasonal Budyko-type model (Eq. (1)) are calibrated to the plots of the prechange period for each season. The calibrated values of n and φ, as well as the corresponding R^2 and RMSE between the plots and fitted curves are summarized in Table 2. Results show that RMSE ranges from 0.01 to 0.04, and R^2 are 0.89, 0.76 and 0.99 for annual scale, irrigation season and energy-limited season, indicating a reasonable performance of the fitting curves. It can be seen that for all seasons the plots for the postchange period are generally distributed on the upper side of the fitting curves, indicating an enhancement of the evaporation ratio $\left(\frac{E}{P-\Delta S}\right)$ and an reduction of streamflow due to direct human interferences. Similar result has been reported by Jaramillo and Destouni (2015) about a flow regulation and irrigation related increase in the ratio of actual evapotranspiration to precipitation at a global scale.

4.3. Parameter estimation of abcd model

As explained in Section 2.2, the abcd model is applied with two main purposes in this study: one is to generate the actual evaporation and water storage change for the prechange and postchange periods for the Budyko decomposition method, and the other is to quantify the impacts of climate change and human impact on streamflow change as a verification of the Budyko decomposition method. For this, parameters of the abcd model are calibrated for both the prechange and postchange periods, thus the corresponding actual evaporation and water storage change can be estimated at the same time as derived by Sankarasubramanian and Vogel (2002). Either period is further divided into a calibration period and a validation period; that is, from 1953 to 1966 (calibration) and 1967 to 1974 (validation) for the prechange period, and from 1975 to 1999 (calibration) and 2000 to 2005 (validation) for the postchange period. The optimized values of model parameters and initial soil water storage are summarized in Table 3.

Fig. 6 displays the simulated and observed monthly streamflow. The performance of the model is generally satisfactory. As shown in Table 4,

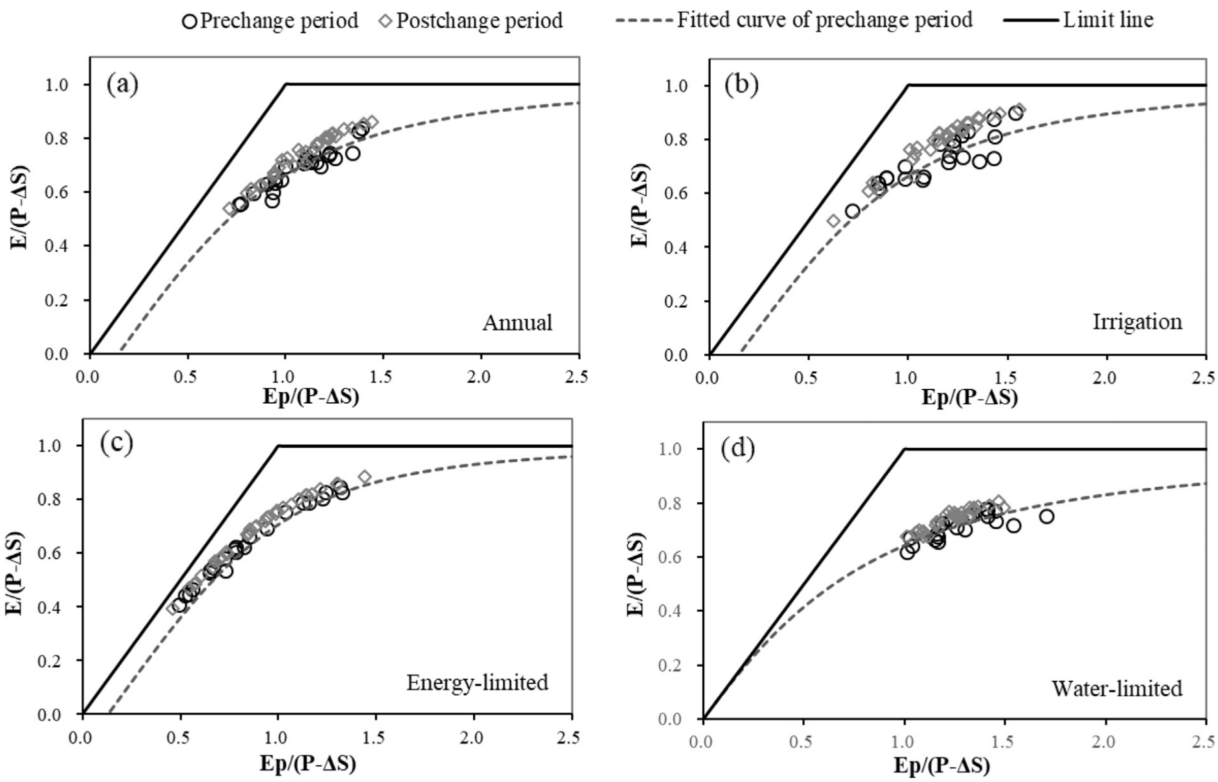

Fig. 5. Correlation between evaporation ratio versus aridity index, and the fitted Budyko-type curves for the prechange period for (a) annual scale, (b) irrigation season, (c) energy-limited season, and (d) water-limited season.

Table 2
Fitting results of the Budyko-type model for the prechange period.

	Parameter		Evaluation index	
	n	φ	R^2	*RMSE*
Annual	2.14	0.14	0.89	0.03
Irrigation season	2.05	0.07	0.76	0.04
Energy-limited season	2.55	0.13	0.99	0.01
Water-limited season	1.58	0.01	0.66	0.03

Table 3
Optimized parameters of abcd model.

Parameter	a	b (mm)	C	d (t^{-1})	Initial soil water storage (mm)
Prechange	0.98	457.36	0.01	0.98	150.81
Postchange	0.99	590.10	0.10	0.99	288.37

NSE and R^2 ranges from 0.75 to 0.86 and 0.71 to 0.87, respectively, indicating a fairly satisfactory fitting condition; thus the model is sufficiently reliable for estimating the hydrological variables for the Budyko decomposition method, as well as for quantifying the relative impacts of climate change and human impacts on streamflow.

4.4. Quantification of climate and direct human impacts on streamflow

The proposed decomposition method based on Budyko-type model is applied to quantify the impacts of climate change and direct human activities on annual and seasonal streamflow changes; and the quantification results are further compared with the abcd model. Fig. 7(a)–(d) presents the quantification results for annual scale, irrigation season, energy-limited season, and water-limited season, respectively; each contains the results from two E_p estimates to account for the uncertainty of E_p and the propagated effect of carrying the abcd model estimates to the Budyko decomposition method. For a specific E_p, the results generated by the Budyko-type model and abcd model agree well. Both climate variability and direct human activity contributed to the decrease of streamflow at the annual scale. At the seasonal scale, direct human activities were found to cause a streamflow decrease for all seasons; whereas climate change led to a streamflow decrease for energy-limited and water-limited seasons, and a streamflow increase for the irrigation period. Although the Budyko decomposition method and abcd model suggested the same ways (increase or decrease) of climate variability and direct human activities in influencing the streamflow change, there were still differences in terms of magnitude. The differences were particularly significant for the irrigation period, with the absolute differences calculated at 3.5 mm/month by averaging two E_p methods, for both climate-induced and direct human-induced changes. Such systematic discrepancy can be attributed to the different calculation procedures and different model structures of the two methods. For example, the abcd model computes the surface runoff and base flow independently; whereas the Budyko method only computes the total runoff.

The contribution of climate change to streamflow change for all seasons can be explained by the changes in effective precipitation and potential evaporation from prechange to postchange periods. For example, the climate-induced increase in streamflow during irrigation season is associated with the increased effective precipitation and decreased potential evaporation. The human-induced streamflow decrease in irrigation season is primarily due to water withdrawals for irrigation. In the energy-limited season, the human interference causes a streamflow decrease by −6.0 mm/month on average. This can be primarily attributed to the constructed ponds and reservoirs for directly storing water during flood seasons; moreover, the stored water potentially signifies higher probability for evaporation due to the larger water surface area (Jaramillo and Destouni, 2015; Maarten et al., 2011). The impact of direct human activities on streamflow change in the water-limited season is relatively small; the decrease in streamflow

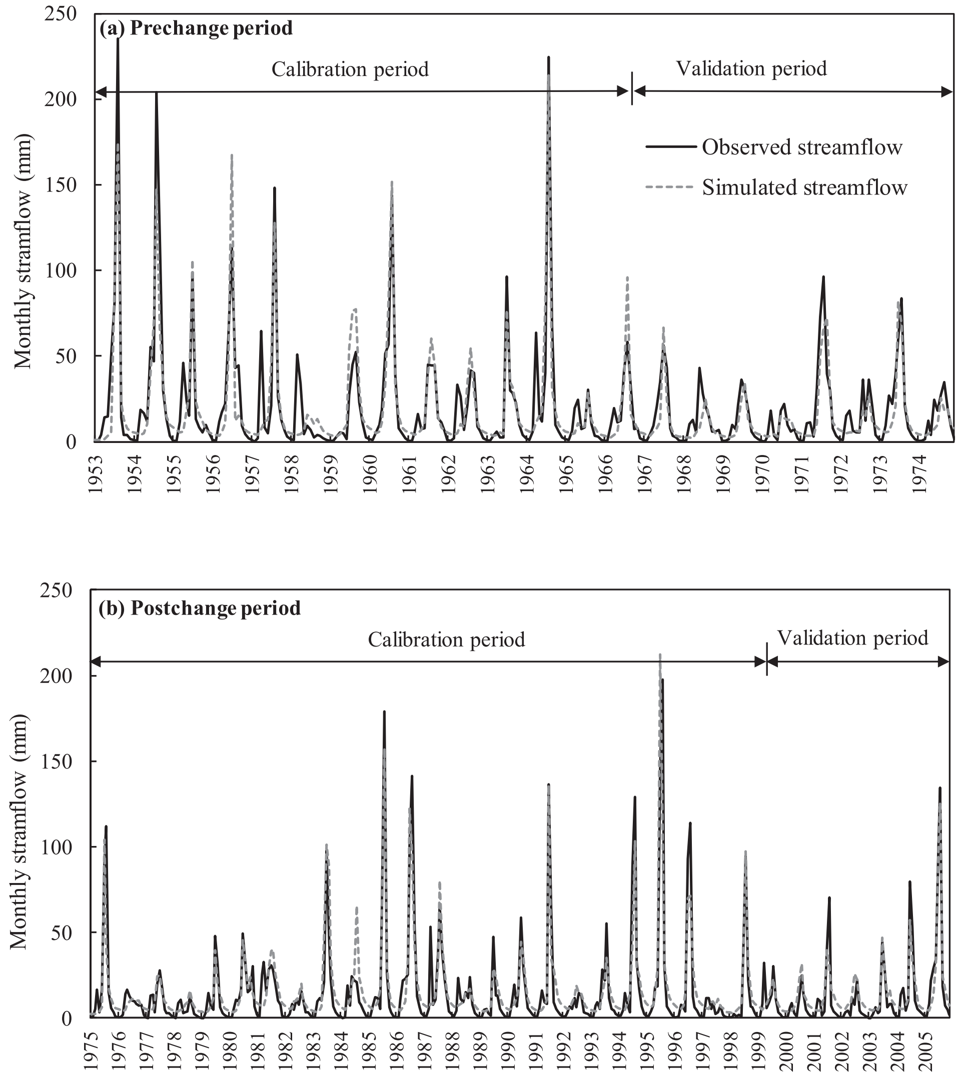

Fig. 6. Results of simulated streamflow by abcd model for (a) prechange period, and (b) postchange period.

Table 4
Performance of abcd model for monthly streamflow simulation.

	NSE	R^2	*NSE*	R^2
Prechange	Calibration (1953–1966)		Validation (1967–1974)	
	0.82	0.82	0.75	0.71
Postchange	Calibration (1975–1999)		Validation (2000–2005)	
	0.80	0.79	0.86	0.87

is primarily due to water withdrawal for domestic use. Note that the quantification results based on two different E_p estimates showed consistent ways (increase or decrease) in influencing the streamflow change; and the magnitude of change are similar except for the irrigation season. Therefore, it can be concluded from the quantification results that human activities play a dominant role in reducing streamflow, especially during the irrigation and energy-limited seasons.

4.5. *Effects of intensive human activities on streamflow in energy-limited season*

The human interferences during the energy-limited season are influential due to flood control facilities and reservoir operations. The operation rules for ponds and reservoirs in each month are illustrated in Fig. 8; correspondingly, the monthly quantification results from the abcd model are shown in Fig. 9. The estimated climate-induced streamflow changes by averaging two E_p results are 22.4 mm, −19.8 mm and −13.6 mm for July, August and September, respectively. Such climate-induced changes are basically resulted from the changes in effective precipitation and potential evaporation. Human activities during this period can be divided into several stages according to operation rules for flood control. Ponds are either empty or with a minimum water level before the flood season (i.e., the end of water-limited season); reservoirs generally need to remain a water level below the flood-limited water level (FLWL) during the entire flood season to maintain adequate storage capacity for flood prevention (Li et al., 2010). During the early stage of the flood season approximately in late July, runoff is largely stored in ponds and reservoirs until the water level reaches FLWL. These filling processes are the primary cause of human-induced streamflow decrease in July. During the middle stage of the flood season (i.e., August), human activities were found to induce an increase in streamflow on average by 4.0 mm/month. This can be explained with two possible reasons. First, the storage in ponds becomes full quickly in the early filling stage since the storage capacities are usually small, and then inflows will be spilled and high inflows may even break the ponds (Cao et al., 2011; Peng et al., 2016). Second, the reservoirs will store water at the water-rising stage temporarily to alleviate the flood damage risk; then the carry-over storage (i.e., the amount above FLWL) will be released during the flood recession period.

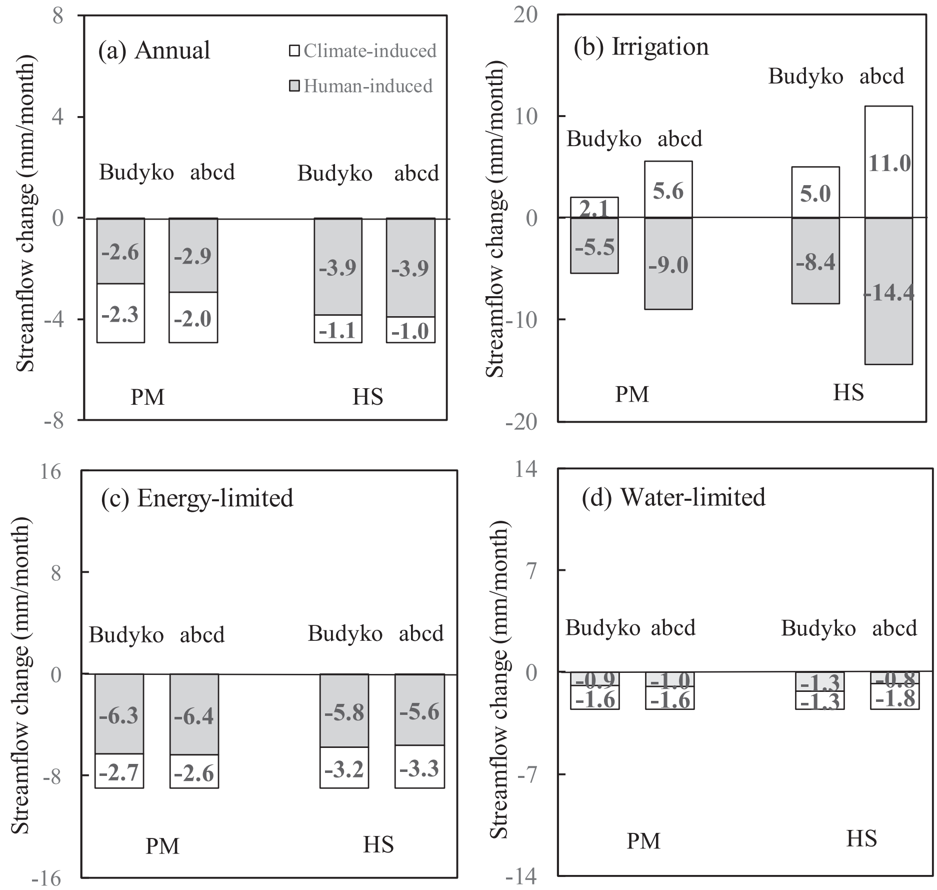

Fig. 7. Quantification results of the climate-induced and direct human-induced changes in streamflow with E_p estimated by the PM and HS methods (numbers in the columns indicate the amount of streamflow change in mm/month).

At the late stage of the flood season (i.e., late August and September), pond storage reaches the storage capacity; while reservoirs store water to the normal water level for future water use, causing a streamflow decrease by −3.8 mm on average in September. This provides useful implications for water conservation under the cascade development. At the end of flood season, the downstream reservoirs can store water in advance under the premise of acceptable flood risk, since the streamflow from upstream may be reduced due to water storage by the upstream reservoirs.

4.6. Potential effects of other possible drivers on streamflow change

This study showed the dominating effects of reservoir operation and irrigation water withdrawals on the water cycles; however, there are

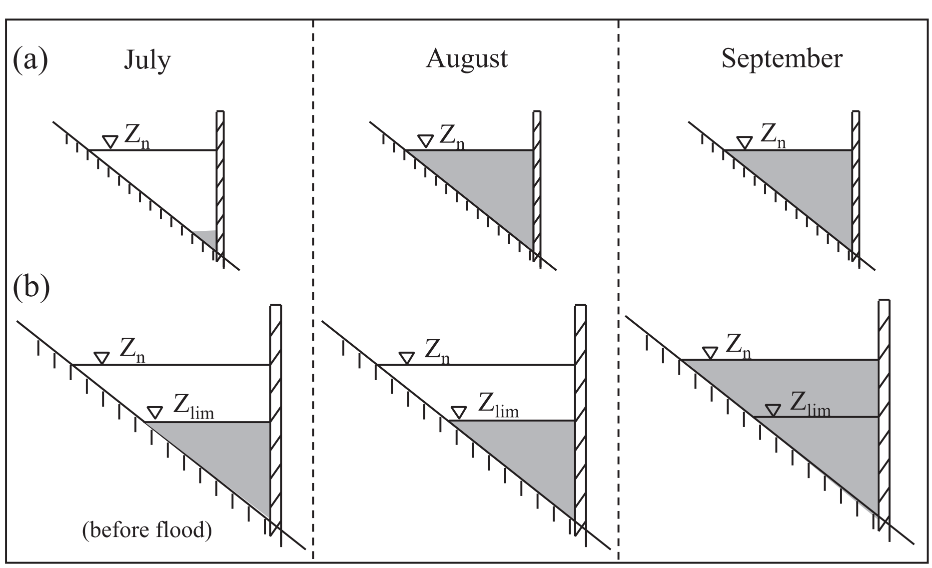

Fig. 8. Sketch of the operation rules for (a) ponds and (b) reservoirs from July to September (grey fillings indicate water storage, Z_{lim} is the flood-limited water level which is the maximum allowed water level during the flood season, Z_n is the normal water level for storage).

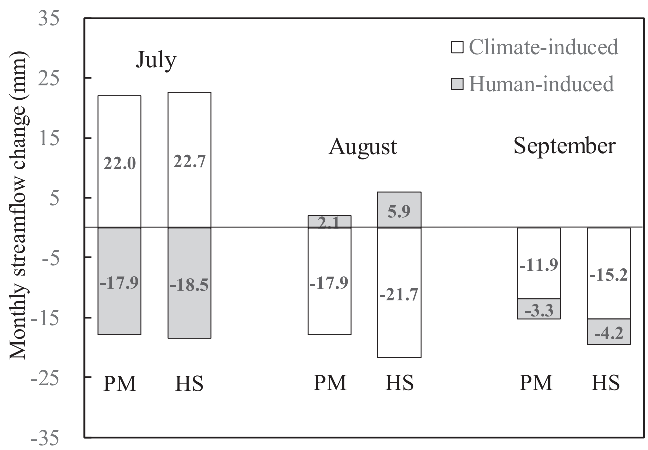

Fig. 9. Quantification results of the climate-induced and human-induced changes in streamflow for each month during the energy-limited season with E_p estimated by the PM and HS methods.

uncertainties on other possible drivers of change on evaporation ratio and streamflow. Changes in forest biomass and vegetation dynamics were among the most influential processes that alter the partitioning of precipitation (Donohue et al., 2012; Jaramillo et al., 2018; Sun et al., 2005; Yang et al., 2008b). The forest clear-cutting could reduce evapotranspiration and increase runoff; whereas reforestation or regrowth has resulted in an opposite effect (Andréassian, 2004; Sørensen et al., 2009). Studies have found the elevated carbon dioxide (CO_2)-driven changes on hydrological cycle via forest or vegetation feedbacks, including the increase in evapotranspiration due to increased leaf area and rooting depth (Bond and Midgley, 2012; Piao et al., 2007), and the decrease in evapotranspiration induced by a water-saving response due to reduced stomata conductance (Betts et al., 2007; Milly and Dunne, 2016; Swann et al., 2016). Studies in China have reported significant impacts of land use/cover changes on evaporation variations depending on the corresponding changes of land use/cover types (Liu et al., 2008; Qiu et al., 2011; Xu et al., 2013). However, this may not apply to the Huifa River basin, which had experienced little human-induced land cover change during the study period (Zhang, 2013). Since the coupled human, climate, and hydrological processes are complicated and interacted, separation of climate change and human impacts on streamflow remains a challenge. Further considerations could be given to quantify the impacts of specific human activities, such as land use change, water withdrawal and return flow.

5. Conclusions

Quantifying the relative impacts of climate change and human activities on streamflow changes at the seasonal/monthly scale is essential due to the intra-annual variations of climate variables and human activities. In this study, the decomposition method based on the Budyko equation is extended to the seasonal scale. Given the simplicity of the proposed method, it is feasible to separate the climate and direct human contributions to seasonal streamflow changes independently with less data required and a lower simulation burden. The seasonal decomposition method can be easily applied to any watersheds if precipitation, potential evaporation, actual evaporation, and runoff data are available.

The proposed decomposition method is applied to the Huifa River basin in China, and the quantification results of the Budyko-type method are verified with the monthly abcd model. Both climate change and direct human activities were found to induce a decrease in streamflow at the annual scale. At the seasonal scale, direct human activities accounted for 67% and 39% on average of the streamflow decrease in the energy-limited and water-limited seasons, respectively; whereas the effect was even pronounced during the irrigation season due to irrigated water withdrawal. The monthly attribution analysis further showed that the operation rules of ponds and reservoirs are influential in altering the streamflow during all stages of flood season. The findings in this study highlight the responses of streamflow as a consequence of intra-annual variations of climate variability and direct human activities, which needs to be thoughtfully considered in water planning and allocation for maintaining a sustainable water resources.

Acknowledgements

This research is supported by the National Key Research and Development Program of China (Grant No. 2017YFC0406001) and the National Natural Science Foundation of China (Grant No. 91647201, 51809031).

Declaration of interests

None.

References

Alley, W.M., 1984. On the treatment of evapotranspiration, soil moisture accounting, and aquifer recharge in monthly water balance models. Water Resour. Res. 20 (8), 1137–1149.
Allen, R.G., Pereira, L.S., Raes, D., Smith, M., 1998. Crop evapotranspiration: guidelines for computing crop water requirements. Food Agric. Org., Rome.
Andréassian, V., 2004. Waters and forests: from historical controversy to scientific debate. J. Hydrol. 291, 1–27.
Arora, V.K., 2002. The use of the aridity index to assess climate change effect on annual runoff. J. Hydrol. 265 (1), 164–177.
Arrigoni, A.S., Greenwood, M.C., Moore, J.N., 2010. Relative impact of anthropogenic modifications versus climate change on the natural flow regimes of rivers in the Northern Rocky Mountains, United States. Water Resour. Res. 46 (12), W12542.
Bao, Z., Zhang, J., Wang, G., Fu, G., He, R., Yan, X., Jin, J., Liu, Y., Zhang, A., 2012. Attribution for decreasing streamflow of the Haihe River basin, northern China: climate variability or human activities? J. Hydrol. 460, 117–129.
Betts, R.A., Boucher, O., Collins, M., Cox, P.M., Falloon, P.D., Gedney, N., Hemming, D.L., Huntingford, C., Jones, C.D., Sexton, D.M.H., Webb, M.J., 2007. Projected increase in continental runoff due to plant responses to increasing carbon dioxide. Nature 448, 1037–1041. https://doi.org/10.1038/nature06045.
Budyko, M.I., 1974. Climate and Life. Academic, New York.
Bond, W.J., Midgley, G.F., 2012. Carbon dioxide and the uneasy interactions of trees and savannah grasses. Philos. Trans. R. Soc. London B. 367 (1588), 601–612. https://doi.org/10.1098/rstb.2011.0182.
Braithwaite, R.J., Zhang, Y., 2000. Sensitivity of mass balance of five Swiss glaciers to temperature changes assessed by tuning a degree-day model. J. Glac. 46 (152), 7–14.
Cao, M., Zhou, H., Zhang, C., Zhang, A., Li, H., Yang, Y., 2011. Research and application of flood detention modeling for ponds and small reservoirs based on remote sensing data. Sci. China Technol. Sc. 54 (8), 2138–2144.
Chen, X., Alimohammadi, N., Wang, D., 2013. Modeling interannual variability of seasonal evaporation and storage change based on the extended Budyko framework. Water Resour. Res. 49, 1–12.
Choudhury, B.J., 1999. Evaluation of an empirical equation for annual evaporation using field observations and results from a biophysical model. J. Hydrol. 216, 99–110.
Dey, P., Mishra, A., 2017. Separating the impacts of climate change and human activities on streamflow: a review of methodologies and critical assumptions. J. Hydrol. 548, 278–290.
Donohue, R.J., Roderick, M.L., McVicar, T.R., 2010. Can dynamic vegetation information improve the accuracy of Budyko's hydrological model? J. Hydrol. 390 (1), 23–34.
Donohue, R.J., Roderick, M.L., McVicar, T.R., 2012. Roots, storms and soil pores: Incorporating key ecohydrological processes into Budyko's hydrological model. J. Hydrol. 436, 35–50. https://doi.org/10.1016/j.jhydrol.2012.02.033.
Dooge, J.C.I., 1992. Sensitivity of runoff to climate change: a Hortonian approach. Bull. Am. Meteorol. Soc. 73 (12), 2013–2024.
Dooge, J.C.I., Bruen, M., Parmentier, B., 1999. A simple model for estimating the sensitivity of runoff to long-term changes in precipitation without a change in vegetation. Adv. Water Resour. 23 (2), 153–163.
Fernandez, W., Vogel, R.M., Sankarasubramanian, A., 2000. Regional calibration of a watershed model. Hydrol. Sci. J. 45 (5), 689–707.
Fu, G., Charles, S.P., Chiew, F.H.S., 2007. A two-parameter climate elasticity of streamflow index to assess climate change effects on annual streamflow. Water Resour. Res. 43, W11419.
Hargreaves, G.H., Samani, Z.A., 1985. Reference crop evapotranspiration from temperature. Appl. Engin. Agric. 1 (2), 96–99.
Hock, R., 2003. Temperature index melt modelling in mountain areas. J. Hydrol. 282, 104–115.
Hock, R., 2005. Glacier melt: a review of processes and their modelling. Progress Phys. Geog. 29 (3), 362–391.

Jaramillo, F., Cory, N., Arheimer, B., Laudon, H., van der Velde, Y., Hasper, T.B., Teutschbein, C., Uddling, J., 2018. Dominant effect of increasing forest biomass on evapotranspiration: interpretations of movement in Budyko space. Hydrol. Earth Syst. Sci. 22 (1), 567–580. https://doi.org/10.5194/hess-22-567-2018, 2018.
Jaramillo, F., Destouni, G., 2014. Developing water change spectra and distinguishing change drivers worldwide. Geophys. Res. Lett. 41 (23), 8377–8386. https://doi.org/10.1002/2014GL061848, 2014.
Jaramillo, F., Destouni, G., 2015. Local flow regulation and irrigation raise global human water consumption and footprint. Science 350 (6265), 1248–1251. https://doi.org/10.1126/science.aad1010.
Jiang, C., Xiong, L., Wang, D., Liu, P., Guo, S., Xu, C.Y., 2015. Separating the impacts of climate change and human activities on runoff using the Budyko-type equations with time-varying parameters. J. Hydrol. 522, 326–338.
Jones, J., 2011. Hydrologic responses to climate change: considering geographic context and alternative hypotheses. Hydrol. Process. 25, 1996–2000.
Kendall, M.G., 1975. Rank Correlation Measures. Charles Griffin, London.
Kundzewicz, Z.W., Mata, L.J., Arnell, N.W., Döll, P., Jimenez, B., Miller, K., Oki, T., Sen, Z., Shiklomanov, I., 2008. The implications of projected climate change for freshwater resources and their management. Hydrol. Sci. J. 53 (1), 3–10.
Li, X., Guo, S., Liu, P., Chen, G., 2010. Dynamic control of flood limited water level for reservoir operation by considering inflow uncertainty. J. Hydrol. 391, 124–132.
Li, Z., Liu, W.Z., Zhang, X.C., Zheng, F.L., 2009. Impacts of land use change and climate variability on hydrology in an agricultural catchment on the Loess Plateau of China. J. Hydrol. 377, 35–42.
Liang, W., Bai, D., Wang, F., Fu, B., Yan, J., Wang, S., Yang, Y., Long, D., Feng, M., 2015. Quantifying the impacts of climate change and ecological restoration streamflow changes based on a Budyko hydrological model in China's Loess Plateau. Water Resour. Res. https://doi.org/10.1002/2014WR016589.
Liu, M., Tian, H., Chen, G., Ren, W., Zhang, C., Liu, J., 2008. Effects of land-use and land-cover change on evapotranspiration and water yield in China during 1900–2001. J. Amer. Water Resour. Assoc. 44 (5), 1193–1207. https://doi.org/10.1111/j.1752-1688.2008.00243.x.
Liu, Y., Zhang, X., Xia, D., You, J., Rong, Y., Bakir, M., 2013. Impacts of land-use and climate changes on hydrologic processes in the Qingyi River watershed. China. J. Hydrol. Eng. 1495–1512.
Ma, H., Yang, D., Tan, S.K., Gao, B., Hua, Q., 2010. Impact of climate variability and human activity on streamflow decrease in the Miyun Reservoir catchment. J. Hydrol. 389, 317–324.
Maarten, S.K., Marjella, J.D., Pieter, R.V., José Carlos, D.A., 2011. Sustainability of small reservoirs and large scale water availability under current conditions and climate change. Water Resour. Manage. 25, 3017–3026.
Mango, L.M., Melesse, A.M., McClain, M.E., Gann, D., Setegn, S., 2011. Land use and climate change impacts on the hydrology of the upper Mara River Basin, Kenya: results of a modeling study to support better resource management. Hydrol. Earth Syst. Sci. 15 (7), 2245.
Mann, H.B., 1945. Non-parametric tests against trend. Econometrica 13 (3), 245–259.
McLaughlin, S.B., Wullschleger, S.D., Sun, G., Nosal, M., 2007. Interactive effects of ozone and climate on water use, soil moisture content and streamflow in a southern Appalachian forest in the USA. New Phytologist. 174, 125–136.
Mezentsev, V.S., 1955. More on the calculation of average total evaporation. Meteorol. Gidrol. 5, 24–26.
Milly, P.C.D., Betancourt, J., Falkenmark, M., Hirsch, R.M., Kundzewicz, Z.W., Lettenmaier, D.P., Stouffer, R.J., 2008. Stationarity is dead: Whither water management? Science 319, 573–574.
Milly, P.C.D., Dunne, K.A., 2016. Potential evapotranspiration and continental drying. Nat. Clim. Change 6, 946–949. https://doi.org/10.1038/nclimate3046.
Niemann, J.D., Eltahir, E.A.B., 2005. Sensitivity of regional hydrology to climate changes, with application to the Illinois River basin. Water Resour. Res. 41, W07014.
Peng, Y., Chu, J., Sun, X., Zhou, H., Zhang, X., 2016. Flood forecasting that considers the impact of hydraulic projects by an improved TOPMODEL model in the Wudaogou basin, Northeast China. Water Sci. Tech.-W. Sup. 16 (5), 1467–1476.
Pettitt, A.N., 1979. A non-parametric approach to the change-point problem. Appl. Statist. 28 (2), 126–135.
Piao, S., Friedlingstein, P., Ciais, P., de Noblet-Ducoudre, N., Labat, D., Zaehle, S., 2007. Changes in climate and land use have a larger direct impact than rising CO2 on global river runoff trends. P. Natl. Acad. Sci. USA 104, 15242–15247. https://doi.org/10.1073/pnas.0707213104.
Qiu, G.Y., Yin, J., Tian, F., Geng, S., 2011. Effects of the "Conversion of Cropland to Forest and Grassland Program" on the Water Budget of the Jinghe River Catchment in China. J. Environ. Qual. 40 (6), 1745–1755. https://doi.org/10.2134/jeq2010.0263.
Rossi, A., Massei, N., Laignel, B., Sebag, D., Copard, Y., 2009. The response of the Mississippi River to climate fluctuations and reservoir construction as indicated by wavelet analysis of streamflow and suspended-sediment load, 1950–1975. J. Hydrol. 377 (3), 237–244.
Sankarasubramanian, A., Vogel, R.M., 2002. Annual hydroclimatology of the United States. Water Resour. Res. 38 (6). https://doi.org/10.1029/2001WR000619.
Sankarasubramanian, A., Vogel, R.M., Limbrunner, J.F., 2001. Climate elasticity of streamflow in the United States. Water Resour. Res. 37, 1771–1781.
Schaake, J.C., 1990. In: Climate Change and US Water Resources. John Wiley, New York, pp. 177–206.
Searcy, J.K., Hardison, C.H., 1960. Double-mass Curves. U.S. Geological Survey Water Supply Paper.
Sivapalan, M., 2006. Patterns, process and function: Elements of a unified theory of hydrology at the catchment scale. Encyclopedia of Hydrological Sciences. John Wiley & Sons Ltd.
Sørensen, R., Ring, E., Meili, M., Högbom, L., Seibert, J., Grabs, T., Laudon, H., Bishop, K., 2009. Forest harvest increases runoff most during low flows in two boreal stream. Ambio. 38, 357–363.
Sun, G., McNulty, S.G., Lu, J., Amatya, D.M., Liang, Y., Kolka, R.K., 2005. Regional annual water yield from forest lands and its response to potential deforestation across the Southeastern United States. J. Hydrol. 308, 258–268.
Sun, S., Chen, H., Ju, W., Song, J., Zhang, H., Sun, J., Fang, Y., 2013. Effects of climate change on annual streamflow using climate elasticity in Poyang Lake Basin. China. Theor. Appl. Climatol. 112 (1–2), 169–183.
Sun, Y., Tian, F., Yang, L., Hu, H., 2014. Exploring the spatial variability of contributions from climate variation and change in catchment properties to streamflow decrease in a mesoscale basin by three different methods. J. Hydrol. 508, 170–180.
Swann, A.L.S., Hoffman, F.M., Koven, C.D., Randerson, J.T., 2016. Plant responses to increasing CO2 reduce estimates of climate impacts on drought severity. P. Natl. Acad. Sci. U.S.A. 113, 10019–10024. https://doi.org/10.1073/pnas.1604581113.
Tang, Q., Lettenmaier, D.P., 2012. 21st century runoff sensitivities of major global river basins. Geophys. Res. Lett. 39, L06403.
Thomas, H.A., 1981. Improved Methods for National Water Assessment. Water Resour. Council, Washington, D.C, pp. 1–59.
Vaze, J., Davidson, A., Teng, J., Podger, G., 2011. Impact of climate change on water availability in the Macquarie-Castlereagh River Basin in Australia. Hydrol. Process. 25 (16), 2597–2612.
Vogel, R.M., 2011. Hydromorphology. J. Water Resour. Plann. Manage. 137 (2), 147–149.
Wang, D., 2012. Evaluating interannual water storage changes at water-sheds in Illinois based on long-term soil moisture and groundwater level data. Water Resour. Res. 47, W00J12. https://doi.org/10.1029/2010WR010283.
Wang, D., Cai, X., 2010. Comparative study of climate and human impacts on seasonal base flow in urban and agricultural watersheds. Geophys. Res. Lett. 37, L06406.
Wang, D., Hejazi, M., 2011. Quantifying the relative contribution of the climate and direct human impacts on mean annual streamflow in the contiguous United States. Water Resour. Res. 47, W00J12.
Wang, D., Tang, Y., 2014. A one parameter Budyko model for water balance captures emergent behavior in darwinian hydrologic models. Geophys. Res. Lett. 41. https://doi.org/10.1002/2014GL060509.
Wang, D., Wu, L., 2013. Similarity of climate control on base flow and perennial stream density in the Budyko framework. Hydrol. Earth Syst. Sci. 17, 315–324.
Wang, G., Xia, J., Chen, J., 2009. Quantification of effects of climate variations and human activities on runoff by a monthly water balance model: a case study of the Chaobai River basin in northern China. Water Resour. Res. 45, W00A11. https://doi.org/10.1029/2007WR006768.
Wang, W., Shao, Q., Yang, T., Peng, S., Xing, W., Sun, F., Luo, Y., 2013. Quantitative assessment of the impact of climate variability and human activities on runoff changes: a case study in four catchments of the Haihe River Basin. China. Hydrol. Process. 27 (8), 1158–1174.
Wu, L., Li, H., Wang, L., 2011. Application of a degree-day model for determination of mass balance of Urumqi Glacier No.1, eastern Tianshan. China. J. Earth Sci. 22 (4), 470–481.
Xu, X., Yang, D., Yang, H., Lei, H., 2014. Attribution analysis based on the Budyko hypothesis for detecting the dominant cause of runoff decline in Haihe basin. J. Hydrol. 510, 530–540.
Xu, X., Yang, H., Yang, D., Ma, H., 2013. Assessing the impacts of climate variability and human activities on annual runoff in the Luan River basin, China. Hydrol. Res. 44 (5), 940–952.
Xue, L., Yang, F., Yang, C., Chen, X., Zhang, L., Chi, Y., Yang, G., 2017. Identification of potential impacts of climate change and anthropogenic activities on streamflow alterations in the Tarim River Basin, China. Sci. Rep. 7 (8254). https://doi.org/10.1038/s41598-017-09215-z.
Yang, Q., 2015. Study on spatio-temporal distribution of snow cover in northeast China and its simulation on snowmelt runoff. Doctoral Dissertation (in Chinese).
Yang, D., Sun, F., Liu, Z., Cong, Z., Ni, G., Lei, Z., 2007. Analyzing spatial and temporal variability of annual water-energy balance in nonhumid regions of China using the Budyko hypothesis. Water Resour. Res. 43, W04426.
Yang, H., Yang, D., 2011. Derivation of climate elasticity of runoff to assess the effects of climate change on annual runoff. Water Resour. Res. 47, W07526.
Yang, H., Yang, D., Lei, Z., Sun, F., 2008a. New analytical derivation of the mean annual water-energy balance equation. Water Resour. Res. 44, W03410. https://doi.org/10.1029/2007WR006135.
Yang, H., Yang, D., Lei, Z., Lei, H., 2008b. Derivation and validation of watershed coupled water-energy balance equation at arbitrary time scale. J. Hydroelectric Eng. 39 (5), 610–617 (in Chinese).
Zhang, A., 2013. Research on the streamflow responses to climate variability and human activities in Northeast China. Doctoral Dissertation (in Chinese).
Zhang, C., Peng, Y., Chu, J., Shoemaker, C.A., Zhang, A., 2012. Integrated hydrological modelling of small-and medium-sized water storages with application to the upper Fengman Reservoir Basin of China. Hydrol. Earth Syst. Sci. 16 (11), 4033–4047.
Zhang, J., Wang, G., 2014. Quantitative identification of river runoff change and its attribution. Science Press, Beijing (in Chinese).